Spin superconductor in ferromagnetic graphene

Qing-feng Sun,[1,*] Zhao-tan Jiang,[2] Yue Yu,[3] and X. C. Xie[4,1]
[1]*Institute of Physics, Chinese Academy of Sciences, Beijing 100190, China*
[2]*Department of Physics, Beijing Institute of Technology, Beijing 100081, China*
[3]*Institute of Theoretical Physics, Chinese Academy of Sciences, Beijing 100190, China*
[4]*International Center for Quantum Materials, Peking University, Beijing 100871, China*
(Received 7 November 2011; published 2 December 2011)

We show a spin superconductor in ferromagnetic graphene as the counterpart to the charge superconductor in which a spin-polarized electron-hole pair plays the role of the spin $2(\hbar/2)$ "Cooper pair" with a neutral charge. We present a BCS-type theory for the spin superconductor. With the "London-type equations" of the super-spin-current density, we show the existence of an electric "Meissner effect" against a spatial varying electric field. We further study a spin superconductor/normal conductor/spin superconductor junction and predict a spin-current Josephson effect.

DOI: 10.1103/PhysRevB.84.214501 PACS number(s): 72.80.Vp, 72.25.−b, 74.20.Fg, 74.50.+r

I. INTRODUCTION

Superconductivity was discovered about a century ago.[1] Since then, it has been one of the central subjects in physics.[1] Many fascinating properties of superconductors, such as zero resistance,[1] the Meissner effect,[2] and the Josephson effect,[3] have many applications nowadays. On the other hand, the potential application of the spin degrees of freedom of an electron, the field of spintronics, is still rapidly developing and is emerging as a major field in condensed matter physics.[4]

The key physics of superconductivity was well understood in the BCS theory[5]: Electrons in a solid state system may have a net weak attraction so that they form Cooper pairs which can then condense into the BCS ground state. The simplest s-wave Cooper pairs are of electric charge $2e$ and spin singlet. A dual of superconductor is the so-called exciton condensate in which a Cooper pair-like object is a particle-hole pair which is charge neutral while its spin may either be singlet or triplet. We name a spin-triplet exciton condensate as the spin superconductor. The exciton condensates can exist in many physical systems.[6,7] However, a general drawback of the exciton condensate is its instability because of electron-hole (e-h) recombination that lowers the total energy of the system [see Fig. 1(a)]. The typical lifetime of an exciton is restricted from picosecond to nanosecond, and at most limited to the microsecond range.[8–10] It is too short for many meaningful applications. Thus, finding a long-lived exciton gas becomes an important task.

About 35 years ago, Shevchenko and Lozovik and Yudson suggested that the exciton could be realized in a double-layer system,[11,12] in which electrons in one layer and holes in the other are spatially separated by an insulator layer. The insulator barrier is proposed to be thin enough to allow for strong Coulomb interaction between electron and hole while high enough to prevent tunneling and e-h recombination. Then the exciton condensate in the e-h bilayer system has quite a long lifetime and the superfluid ground state can be displayed. Later, the experimental data also show the existence of exciton condensate in the e-h bilayer on semiconductor double quantum well systems.[13,14]

A few year ago, graphene, a single-layer hexagonal lattice of carbon atoms, had been successfully fabricated.[15–18] The unique structure of graphene leads to many peculiar properties, for example, the relativistic-like quasiparticles spectrum.[17,18] Recently, some works have been devoted to the excitons in graphene systems.[19–23] The exciton condensate was suggested in a double-layer graphene system in which the two graphene monolayers are separated by an insulator layer.[19–21] The Kosterlitz-Thouless transition temperature for exciton condensate are estimated and the effect of the screening of the Coulomb interactions on the transition temperature was studied.[19–21] In addition, the possibility of excite condensate in a monolayer undoped graphene was also investigated.[22,23] A detailed theory of this issue has been developed in Ref. 23. However, in all previous works, the exciton is spin unpolarized, and the spin-polarized triplet exciton (i.e., the spin superconductor state) is never mentioned.

For graphene, the charge carriers are usually spin unpolarized. However, if graphene is growing on a ferromagnetic (FM) material[24–26] or is under an external magnetic field,[27] a spin split M can be induced. Then the carriers are spin polarized and the Dirac points with different spins are split. When the Fermi level lies in between the spin-resolved Dirac points [see Fig. 1(b)], the spin-up carriers are electron-like while the spin-down ones are hole-like. These positive and negative carriers attract and form e-h pairs that are stable against the e-h recombination due to the Coulomb interaction. This is because the filled electron-like states are now below the hole-like states, as shown in Fig. 1(b), unlike in conventional exciton systems in semiconductors [Fig. 1(a)] where the electron states are above the hole states. If a carrier jumps from the electron-like state to the hole-like one, the total energy of the system rises. This prevents the e-h recombination and means the e-h pairs in FM graphene is stable and can exist indefinitely in principle. Therefore, this e-h pair gas can condense.

In this work we show that this condensate is a spin superconductor. The spin superconductor is an (charge) insulator and (charge) current cannot flow through it. But its spin resistance is zero and the spin current can dissipationlessly flow in it. We present a BCS-type theory for the spin superconductor, and derive the London-type equations of the super-spin current and find an electric "Meissner effect" against the spatial variation of an electric field. Furthermore, a spin superconductor/normal conductor/spin superconductor junction is studied and a

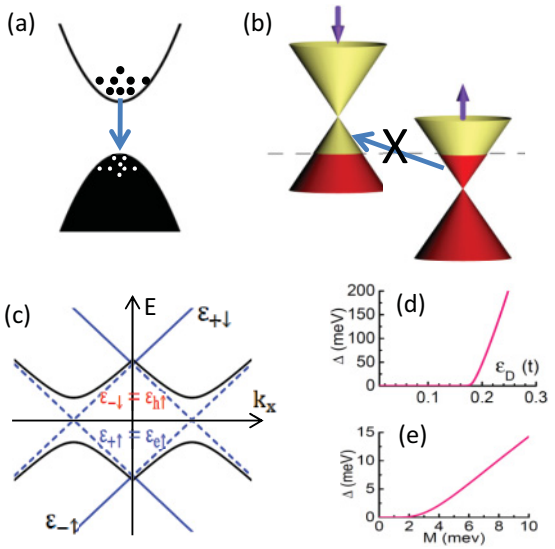

FIG. 1. (Color online) The schematic diagrams: (a) the band structure for the conventional exciton system and (b) for FM graphene. (c) The schematic energy bands of FM graphene for free electrons (blue curves) and for the e-h pair condensate (black curves). (d) The gap Δ vs ϵ_D at the FM magnetic moment $M = 5$ meV and (e) the gap vs M at $\epsilon_D = 0.18t$.

spin-current Josephson effect is predicted. Finally, how to detect the spin superconductor state is discussed and a feasible experiment setup is suggested.

The remainder of this paper is organized as follows. In Sec. II we describe the model and present a BCS-type theory for the spin superconductor. In Sec. III we derive the London-type equation of the super-spin current and show the electric Meissner effect. We study the spin-current Josephson effect in Sec. IV. Section V is devoted to the detection of the spin superconductor. Finally, the conclusion is presented in Sec. VI. Some auxiliary materials are relegated into an Appendix.

II. MODEL AND BCS-TYPE THEORY FOR THE SPIN SUPERCONDUCTOR

We consider an interacting electron system in graphene with the Hamiltonian $H = H_0 + U_C$, where H_0 is the free Dirac fermion Hamiltonian and U_C is the electron-electron (e-e) Coulomb interaction:

$$H_0 = \sum_{\mathbf{k},\sigma} \Psi^\dagger_{\mathbf{k}\sigma} \begin{pmatrix} -\sigma M & v_F(k_x - ik_y) \\ v_F(k_x + ik_y) & -\sigma M \end{pmatrix} \Psi_{\mathbf{k}\sigma},$$
$$U_C = \sum_{s,s';i,j;\sigma,\sigma'} U^{ss'}_{ij} n^s_{i\sigma} n^{s'}_{j\sigma'}, \tag{1}$$

where $\Psi_{\mathbf{k}\sigma} = (a_{\mathbf{k}\sigma}, b_{\mathbf{k}\sigma})^T$, $s_{\mathbf{k}\sigma}$ $(s = a,b)$ are the Fourier components of the electron annihilation operators $s_{i\sigma}$ at sites i for the sublattices s, and $n^s_{i\sigma} = s^\dagger_{i\sigma} s_{i\sigma}$ are the local electron number operators. $\mathbf{k} = (k_x, k_y)$ is the momentum, $\sigma = (\uparrow, \downarrow)$ represents the spin, M is the FM exchange split energy, $U^{ss'}_{ij}$ is the e-e Coulomb potential, and $v_F = 3ta_0/2$ with the nearest hopping energy t and the carbon-carbon distance a_0. Here we have ignored the valley degree of freedom, because the two valleys are degenerate and the intervalley coupling is normally very weak due to the two valleys being well separated in k space. Hereafter we also set the Fermi energy E_F at zero. By taking a unitary transformation: $a_{\mathbf{k}\sigma} = \sum_\tau \tau c^* \alpha_{\mathbf{k}\tau\sigma}$ and $b_{\mathbf{k}\sigma} = \sum_\tau c\alpha_{\mathbf{k}\tau\sigma}$ with the pseudospin index $\tau = \pm$, $c = e^{i\theta/2}/\sqrt{2}$ and $\theta = \tan^{-1}(k_y/k_x)$, the free Hamiltonian H_0 can be diagonalized $H_0 = \sum_{\mathbf{k},\tau,\sigma} \epsilon_{\tau\sigma} \alpha_{\mathbf{k}\tau\sigma} \alpha^\dagger_{\mathbf{k}\tau\sigma}$, where $\epsilon_{\tau\sigma} = -\sigma M + \tau v_F k$ $(k = |\mathbf{k}| = \sqrt{k_x^2 + k_y^2})$ are four energy bands [see the blue curves in Fig. 1(c)] because the spin degeneracy is lifted now. While $E_F = 0$, $\epsilon_{-\uparrow}$ and $\epsilon_{+\downarrow}$ are high-energy bands. In the following, we focus on the low-energy part and only two bands $\epsilon_{+\uparrow}$ and $\epsilon_{-\downarrow}$ are involved. Here the band $\epsilon_{+\uparrow}$ is electron-like, while the band $\epsilon_{-\downarrow}$ is hole-like and the annihilation operator $\alpha_{\mathbf{k}-\downarrow}$ also means to create a spin-up hole. Thus we define operators $\alpha_{\mathbf{k}e\uparrow} = \alpha_{\mathbf{k}+\uparrow}$ and $\alpha^\dagger_{\mathbf{k}h\uparrow} = \alpha_{\mathbf{k}-\downarrow}$. The Hamiltonian H_0 can then be written as

$$H_0 = \sum_{\mathbf{k}} (\alpha^\dagger_{\mathbf{k}e\uparrow}, \alpha_{\mathbf{k}h\uparrow}) \begin{pmatrix} \epsilon_{+\uparrow} & 0 \\ 0 & \epsilon_{-\downarrow} \end{pmatrix} \begin{pmatrix} \alpha_{\mathbf{k}e\uparrow} \\ \alpha^\dagger_{\mathbf{k}h\uparrow} \end{pmatrix}. \tag{2}$$

For the e-e interaction U_C we also focus on the two low-energy bands which are given by the terms $\alpha^\dagger_{\mathbf{k}-\mathbf{q},e\uparrow} \alpha_{\mathbf{k}e\uparrow} \alpha_{\mathbf{k}'+\mathbf{q},h\uparrow} \alpha^\dagger_{\mathbf{k}'h\uparrow}$. Furthermore, we keep only the terms whose momenta satisfy $\mathbf{k} - \mathbf{q} = \mathbf{k}'$, giving rise to the zero momentum e-h pair that is energetically favorable. Under these approximations, the interaction U_C reduces to the attraction between electrons and holes

$$U_C = -\sum_{\mathbf{k},\mathbf{k}'} U_{\mathbf{k}\mathbf{k}'} \alpha^\dagger_{\mathbf{k}'e\uparrow} \alpha^\dagger_{\mathbf{k}'h\uparrow} \alpha_{\mathbf{k}h\uparrow} \alpha_{\mathbf{k}e\uparrow}, \tag{3}$$

where $U_{\mathbf{k}\mathbf{k}'} = (U^{ab}_{\mathbf{k}\mathbf{k}'} e^{i(\theta'-\theta)} + U^{ab}_{\mathbf{k}'\mathbf{k}} e^{i(\theta-\theta')} + U^{aa}_{\mathbf{k}\mathbf{k}'} + U^{bb}_{\mathbf{k}\mathbf{k}'})/4$ with $U^{ab}_{\mathbf{k}\mathbf{k}'} = \sum_j U^{ab}_{0j} e^{-i(\mathbf{k}-\mathbf{k}')\cdot(\mathbf{r}_j+\delta)}$ and $U^{ss}_{\mathbf{k}\mathbf{k}'} = \sum_j U^{ss}_{0j}$ $e^{-i(\mathbf{k}-\mathbf{k}')\cdot\mathbf{r}_j}$ for the coordinate $\mathbf{r}_j$ of the site j and the lattice spacing vector δ. $U_{\mathbf{k}\mathbf{k}'}$ is a large positive value at $\mathbf{k} = \mathbf{k}'$ and it gradually and oscillatorily decays to zero with increase of $|\mathbf{k} - \mathbf{k}'|$. On the one hand, as discussed in Sec. I and Fig. 1(b), this attractive interaction does not induce the e-h recombination. On the other hand, it leads to the instability of the FM metal state at the low temperature (see the Appendix), so the electrons and holes are bound into pairs. The mean-field approximation of Eq. (3) reads

$$U_C \approx \sum_{\mathbf{k}} \Delta_{\mathbf{k}} \alpha^\dagger_{\mathbf{k}e\uparrow} \alpha^\dagger_{\mathbf{k}h\uparrow} + \sum_{\mathbf{k}} \Delta^*_{\mathbf{k}} \alpha_{\mathbf{k}h\uparrow} \alpha_{\mathbf{k}e\uparrow}$$

with the e-h pair condensation order parameter $\Delta_{\mathbf{k}} \equiv -\sum_{\mathbf{k}'} U_{\mathbf{k}'\mathbf{k}} \langle \alpha_{\mathbf{k}'h\uparrow} \alpha_{\mathbf{k}'e\uparrow} \rangle$.

Compared with the spin singlet Cooper pair with charge $2e$, this e-h pair is of spin $\hbar$ and charge neutral. The total mean-field Hamiltonian then is given by

$$H_{\mathrm{MF}} = \sum_{\mathbf{k}} (\alpha^\dagger_{\mathbf{k}e\uparrow}, \alpha_{\mathbf{k}h\uparrow}) \begin{pmatrix} \epsilon_{+\uparrow} & \Delta_{\mathbf{k}} \\ \Delta^*_{\mathbf{k}} & \epsilon_{-\downarrow} \end{pmatrix} \begin{pmatrix} \alpha_{\mathbf{k}e\uparrow} \\ \alpha^\dagger_{\mathbf{k}h\uparrow} \end{pmatrix}. \tag{4}$$

The energy spectrum for the mean-field Hamiltonian H_{MF} is shown in Fig. 1(c). An energy gap with the magnitude of $|\Delta_{\mathbf{k}}|$ is opened. When an electron and a hole combine into an e-h pair, the energy of the system is reduced by $2|\Delta_{\mathbf{k}}|$. This means the condensed state of the e-h pairs is more stable than the unpaired one. Thus, the ground state of FM graphene is a neutral superfluid with spin $\hbar$ per pair; namely, a spin

superconductor state. The spin current can dissipationlessly flow in the spin superconductor and its spin resistance is zero. On the other hand, because an energy gap opened and the e-h pair is charge neutral, the spin superconductor is an (charge) insulator and the (charge) current cannot flow through it.

The energy gap Δ can be estimated as follows. By using the definition $\Delta_{\mathbf{k}} \equiv -\sum_{\mathbf{k}'} U_{\mathbf{k}'\mathbf{k}} \langle \alpha_{\mathbf{k}'h\uparrow} \alpha_{\mathbf{k}'e\uparrow} \rangle$ and the Hamiltonian $H_{\rm MF}$, one has the self-consistent equation

$$\Delta_{\mathbf{k}} = \sum_{\mathbf{k}'} (U_{\mathbf{k}\mathbf{k}'} \Delta_{\mathbf{k}'}/2A)[f(-A) - f(A)], \tag{5}$$

where $f(A) = 1/[\exp(A/k_B T) + 1]$, $A = \sqrt{(M - k')^2 + \Delta_{\mathbf{k}'}^2}$, and T is the temperature. At zero temperature and assuming $U_{\mathbf{k}\mathbf{k}'} = U\theta(k_D - |\mathbf{k} - \mathbf{k}'|)$ with the cut-off momentum k_D, the self-consistent equation (5) reduces to $1 = (U/2)\sum_{\mathbf{k}} \theta(k_D - k)/\sqrt{(M-k)^2 + \Delta^2} = \frac{\sqrt{3}U}{3t^2} \int_0^{\epsilon_D} d\epsilon_k \frac{2\pi\epsilon_k}{\sqrt{(M-\epsilon_k)^2+\Delta^2}}$, where $\epsilon_D = v_F k_D$. Numerically we solve the self-consistent equation by using the e-e interaction U_C with the nearest neighbor cut off. The gaps vary as the cut-off ϵ_D for a fixed M or as the FM split energy M for a fixed ϵ_D are shown in Figs. 1(d) and 1(e), respectively. We see that the gap Δ grows faster than an exponential function with increase of ϵ_D. When $M = 5$ meV and $\epsilon_D = 0.18t$,[24,25] one gets $\Delta \approx 3$ meV. This yields the critical temperature T_C of the transition from the normal state to the spin superconductor at about 30 K. While $T > T_C$, the FM graphene is in the FM metal state, whereas for $T < T_C$ it is in the spin superconductor state. Similar to the case in a superconductor, in the presence of weak impurities, T_C is slightly reduced but the spin superconductor phase can still exist if $T < T_C$, except in the case when the impurity strength is larger than Δ and its density is higher than $1/\xi^2$ with ξ being the coherence length $\xi = \hbar v_F/\Delta$.

III. LONDON-TYPE EQUATION AND ELECTRIC MEISSNER EFFECT

Meissner effect is the criterion that a superconductor differs from a perfect metal: The magnetic field cannot enter the bulk of a superconductor.[2] This phenomenon can be described by the London equations.[28] Is there a Meissner-like effect for the spin superconductor? Consider a spin superconductor with the superfluid carrier density n_s in an electric field $\mathbf{E}$ and a magnetic field $\mathbf{B}$. A magnetic force $\mathbf{F} = (\mathbf{m} \cdot \nabla)\mathbf{B}$ acts on these spin carriers. Here $\mathbf{m} = (4\pi g \mu_B/h)\mathbf{s}$ is the magnetic moment of a carrier, μ_B is the Bohr magneton, and g is the Lande factor. This force accelerates the carrier by Newton's second law $\mathbf{F} = m^* d\mathbf{v}/dt$ for a carrier with the velocity $\mathbf{v}$ and the effective mass m^*. The spin current density $\mathbb{J}_s = n_s \mathbf{v}\mathbf{s}$ is thus a tensor. The time derivative of this super-spin-current density $\mathbb{J}_s$ is then given by

$$d\mathbb{J}_s/dt = a(\mathbf{s} \cdot \nabla)\mathbf{B}\mathbf{s}, \tag{6}$$

with the constant $a = 4\pi g \mu_B n_s/hm^*$. Comparing with London's first equation for the super-charge-current density[28] $d\mathbf{J}/dt \propto \mathbf{E}$, the spatial variation of $\mathbf{B}$ along with the magnetic moment plays the role of an external field accelerating the spin carriers.

When an electric field $\mathbf{E}$ applies by acting $(\mathbf{s} \cdot \nabla)$ on two sides of the Maxwell equations $\nabla \times \mathbf{B} = \mu_0 \epsilon_0 \partial \mathbf{E}/\partial t$ and using Eq. (6), we obtain $\frac{\partial}{\partial t}[\nabla \times \mathbb{J}_s] = \frac{\partial}{\partial t}[\mu_0 \epsilon_0 a(\mathbf{s} \cdot \nabla)\mathbf{E}\mathbf{s}]$. Integrating over the time t, one has the equation for $\mathbb{J}_s$,

$$\nabla \times \mathbb{J}_s = \mu_0 \epsilon_0 a(\mathbf{s} \cdot \nabla)\mathbf{E}\mathbf{s}, \tag{7}$$

where the integral constant is taken to be zero because of the requirement of thermodynamic equilibrium. Instead of the magnetic field in London's second equation for the superconductor,[28] the "external field" here is the spatial variation of the electric field $\mathbf{E}$ along with the magnetic moment.

Equations (6) and (7) for $\mathbb{J}_s$ play roles similar to the London equations in superconductor.[28] For example, if the system is in the steady state, $d\mathbb{J}_s/dt = a(\mathbf{s} \cdot \nabla)\mathbf{B}\mathbf{s} = 0$ implies that the variation $(\mathbf{s} \cdot \nabla)\mathbf{B}$ of the magnetic field along the direction of the FM magnetic moment $\mathbf{m}$ must be zero because of the zero spin resistance. On the other hand, Eq. (7) means the variation of the electric field $(\mathbf{s} \cdot \nabla)\mathbf{E}$ is zero in bulk of the spin superconductor. This is an electric Meissner effect in the spin superconductor against a spatial variation of an electric field. Notice that it is not against the electric field, because of the magnetic moment $\mathbf{m}$ being a dipole instead of a monopole.

We now give an example of this electric Meissner effect. Consider a positive charge Q at the origin and an infinite FM graphene in the x-y plane at $z = Z$ as shown in Fig. 2(a). The charge Q generates an electric field $\mathbf{E}$ in FM graphene plane. This electric field will induce a super-spin current in graphene against the spatial variation of $\mathbf{E}$. Assuming that the magnetic moment $\mathbf{m}$ (i.e., $\mathbf{s}$) is in the z direction, then $(\mathbf{s} \cdot \nabla)E_z = \partial_z E_z = \frac{Q}{4\pi\epsilon_0} \frac{r^2 - 2z^2}{(z^2+r^2)^{5/2}}$ with $r^2 = x^2 + y^2$. Solving Eq. (7), one has the induced super-spin-current density $J_s = -\frac{\mu_0 a Q}{4\pi} \frac{r}{(Z^2+r^2)^{3/2}}$. This J_s flows along the tangential direction [see Fig. 2(a)] and its spin points to the z direction. On the other hand, as a usual spin current,[29] the super-spin-current density J_s can generate an electric field $\mathbf{E}^i$ in space, which is the same as that generated by the electric dipole moment $\vec{p}_e \propto [-\frac{r}{(Z^2+r^2)^{3/2}}, 0, 0]$ or the equivalent charge $Q_i = -\nabla \cdot \vec{p}_e \propto \frac{2Z^2 - r^2}{(Z^2+r^2)^{5/2}}$. In Fig. 2(b) we plot the radial distributions in graphene for the variation $\partial_z E_z$ of the electric field of the original charge Q, the induced super-spin-current density J_s, and the equivalent charge Q_i (i.e., the spatial variation $\partial_z E_z^i$). For $r < \sqrt{2}Z$ ($r > \sqrt{2}Z$) with $\partial_z E_z$ being negative (positive), the spatial variation $\partial_z E_z^i$ of the electric field $\mathbf{E}^i$ induced by

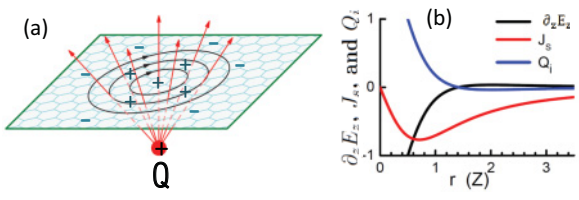

FIG. 2. (Color online) (a) The schematic diagram for the device consisting of a positive charge Q and FM graphene. (b) The variation $\partial_z E_z$ $(Q/4\pi\epsilon_0)$ of the electric field, the induced super-spin-current J_s $(\mu_0 a Q/8\pi)$, and the equivalent charge Q_i (i.e., $\partial_z E_z^i$) vs the radial distance r.

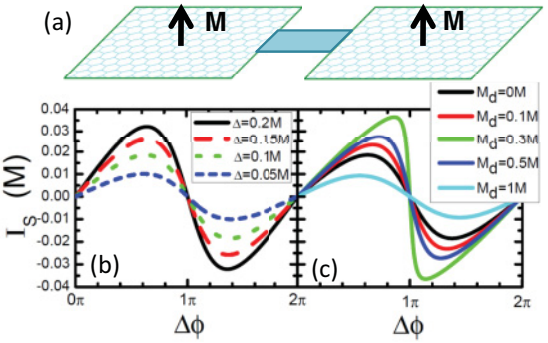

FIG. 3. (Color online) (a) The schematic diagram of the weakly coupled spin superconductor-normal conductor-spin superconductor junction. (b) The spin current I_s vs the phase difference $\Delta\phi$ for different Δ and $M_d = 0$. (c) The I_s-$\Delta\phi$ curves for different M_d and $\Delta = 0.1M$. Here $\epsilon_d = 0$ and $\Gamma \equiv 2\pi t_\beta^2 \rho_k = 0.1M$; ρ_k is the density of state of FM graphene in momentum space.

the super-spin current is positive (negative). As a result, $\partial_z E_z^i$ counteracts the variation $\partial_z E_z$ and then causes the variation of the total electric field in the spin superconductor to vanish.

IV. SPIN-CURRENT JOSEPHSON EFFECT

Josephson effect is another highlight of superconductivity and has wide applications.[3] We now investigate the similar effect for this spin superconductor by considering a device consisting of two spin superconductors, which are weakly coupled by a normal conductor, that is, a spin superconductor/normal conductor/spin superconductor junction [see Fig. 3(a)]. We can explicitly show the existence of the super-spin current in this device in equilibrium. The weakly coupled junction is described by the Hamiltonian $H = \sum_{\beta(\beta=L,R)} H_\beta + H_c + H_T$, where

$$H_\beta = \sum_{\mathbf{k}} (\alpha^\dagger_{\beta\mathbf{k}e\uparrow}, \alpha_{\beta\mathbf{k}h\uparrow}) \begin{pmatrix} \epsilon_{+\uparrow} & \Delta_{\beta\mathbf{k}} \\ \Delta^*_{\beta\mathbf{k}} & \epsilon_{-\downarrow} \end{pmatrix} \begin{pmatrix} \alpha_{\beta\mathbf{k}e\uparrow} \\ \alpha^\dagger_{\beta\mathbf{k}h\uparrow} \end{pmatrix},$$

$$H_c = \sum_\sigma (\epsilon_d + \sigma M_d) c^\dagger_\sigma c_\sigma,$$

$$H_T = \sum_{\beta,\mathbf{k}} [t_\beta \alpha^\dagger_{\beta\mathbf{k}+\uparrow} c_\uparrow + t_\beta \alpha^\dagger_{\beta\mathbf{k}-\downarrow} c_\downarrow + \text{H.c.}].$$

Namely, $H_{L/R}$, H_c, and H_T are the Hamiltonians of the left/right spin superconductor, the normal conductor, and the tunnelings between them, respectively. The order parameters $\Delta_{L/R\mathbf{k}} = \Delta e^{i\phi_{L/R}}$ with the spin superconductor phases $\phi_{L/R}$ are assumed to be independent of the momentum $\mathbf{k}$. We consider a phase difference $\Delta\phi \equiv \phi_L - \phi_R$ between the left and right spin superconductors, which origins from a spin current flowing through the junction under the drive of an external device or from a variation of an external electric field thread the ring junction device. The normal conductor is described by a level (or a quantum dot) with the spin index σ and spin-split energy M_d.

The spin-dependent particle current $I_{\beta\sigma}$ with the spin σ from the β spin superconductor to the central normal conductor can be calculated by the following equation[30]: $I_{\beta\sigma} = \text{Re}(2t^*_\beta/\hbar) \int \frac{d\epsilon}{2\pi} G^<_{\beta\sigma,\sigma}(\epsilon)$, where the lesser Green function $G^<_{\beta\sigma,\sigma}(\epsilon)$ is the Fourier transformation of $G^<_{\beta\sigma,\sigma}(t) \equiv i\langle c^\dagger_\sigma(0)\alpha_{\beta\mathbf{k}\pm\sigma}(t)\rangle$. This Green function $G^<_{\beta\sigma,\sigma}(\epsilon)$ can be calculated by using the Dyson equation and so is the particle current $I_{\beta\sigma}$.[31] Therefore, one can obtain the spin current $I_s = (I_{R\uparrow} - I_{R\downarrow})\hbar/2$ and the charge current $I_e = (I_{R\uparrow} + I_{R\downarrow})e$. The charge current I_e is identically zero because the e-h pairs are charge neutral. The spin current I_s versus $\Delta\phi$ in the equilibrium with zero bias and zero spin bias is calculated and shown in Fig. 3. There is a super-spin current flowing through the junction that resembles the Josephson tunneling in a conventional superconductor junction. While Fig. 3(b) exhibits the I_s-$\Delta\phi$ curves for different values of the gap Δ with $m_d = 0$, Fig. 3(c) shows I_s can also be observed in nonzero M_d as long as $\Delta \neq 0$ and $\Delta\phi \neq 0,\pi$.

V. THE DETECTION OF THE SPIN SUPERCONDUCTOR

In this section we discuss how to detect the spin superconductor state. In the following we first suggest five measurable physical quantities or methods, and then follow up by proposing an experimental setup.

(1) When the system enters the spin superconductor state, an energy gap opens up [see Fig. 1(c)]. This energy gap can be measured by ARPES or STM. When the temperature T is lower (or higher) than T_C, the gap opens (or closes).

(2) Because the spin superconductor is an (charge) insulator, the resistance sharply increases when the FM graphene enters from the normal FM metal state to the spin superconductor state. This sharp increase in resistance can be easily tested in the experiment.

(3) The zero spin resistance is a main characteristic for the spin superconductor. Due to the zero spin resistance, the spin current can flow without any dissipation even for a macroscopic sample. At the end of this section, based on the behavior of the zero spin resistance, we propose a four-terminal device to detect the spin superconductor.

(4) In the electric Meissner effect, an electric field applied to the spin superconductor can induce the super-spin current on the surface of the sample. This induced super-spin current can generate an electric field $\mathbf{E}^i$ that is against the variation of the external electric field. Here the induced electric field $\mathbf{E}^i$ is equivalent to that generated by a certain surface charge distribution. In this case, the induced electric field and the equivalent surface charge distribution are the measurable quantities. For the example of Fig. 2, the equivalent surface charge Q_i is proportional to $\frac{n_s}{m^*}\frac{2Z^2-r^2}{(Z^2+r^2)^{5/2}}$, this value is quite large due to the smallness of the effective mass m^* in graphene. But the equivalent surface charge Q_i is still finite even if $m^* = 0$, since once it reaches the complete shielding and the variation of the total electric field is zero, no more super-spin current and charge are induced. By considering the complete shielding case, the inducing surface charge $Q_i = \frac{2Z^2-r^2}{(Z^2+r^2)^{5/2}}\frac{Qd}{4\pi}$, where $d \approx 0.1$ nm is the thickness of graphene. Let us estimate the value of Q_i. We assume that the distance Z between the external charge Q and the plane of graphene is 10 nm and Q is a basic charge. The inducing surface charge Q_i is about 10^{13} m^{-2} at the position $r = 0$. This surface charge is quite large and should be measurable.

(5) The super spin current in the spin superconductor or in the spin-current Josephson effect is also a measurable physical

quantity. For example, the super-spin current can be directly measured by observing the second-harmonic generation of the Faraday rotation as done in Ref. 32. In addition, many indirect methods have successfully measured the spin current.[33] These methods can also be used in our system. Let us imagine a spin current flowing into the spin superconductor (FM graphene) from one terminal, this spin current can flow through the spin superconductor with no dissipation and flows out from another terminal. Then we can measure the (usual) spin current at the outside through these methods in Ref. 33.

Notice that it is not necessary to do all of the aforementioned measurements. In fact, if one can take a measurement either in 3, 4, or 5, it establishes the presence of the spin superconductor.

In the following, based on the experiment in Ref. 16, here we propose a four-terminal device consisting of a graphene ribbon coupled by four FM electrodes and a long FM strip, as shown in Figs. 4(a) and 4(b), which can be used to measure the nonlocal resistance and then confirm the spin superconductor state. Except for the long FM strip (the red region), the device is what was used in Ref. 16. So this device can be realized by the present technology. The long red strip is a FM insulator which directly couples to the graphene without the Al_2O_3 layer. So the graphene in the red region has a FM exchange splitting and it is normal FM graphene at high temperature and turns to the spin superconductor at low temperature. Now we can qualitatively analyze the measurement results if the spin superconductor is realized. To simplify the analysis, we only consider the magnetic moments in all FM electrodes and strip are in the same direction.

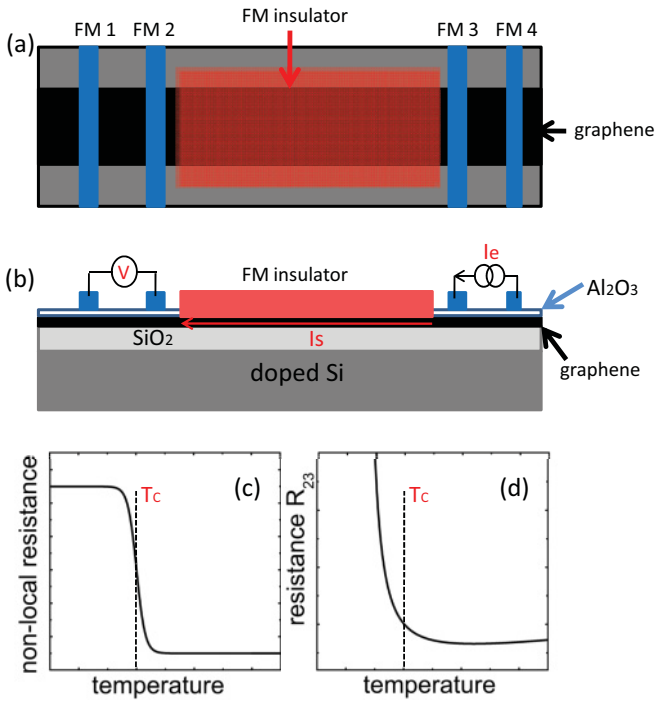

FIG. 4. (Color online) (a) and (b) are schematic diagrams for the proposed device. (a) is the top view and (b) is the side view. (c) and (d) schematically show the nonlocal resistance and the resistance R_{23} vs the temperature, respectively.

Here we measure the nonlocal resistance as in the experiment in Ref. 16. In this measurement a current is applied to the two right electrodes (electrodes 3 and 4) and the bias is measured on the two left electrodes (electrodes 1 and 2). When a current is applied between electrodes 3 and 4, it injects a pure spin current into graphene. This pure spin current flows from electrode 3 through FM graphene (spin superconductor) to the left side [see the Fig. 4(b)]. Then it induces the bias between electrodes 1 and 2. When FM graphene is in the normal FM metal phase, it has a finite spin resistance. In this case, the spin current gradually decays along its transport direction, so the bias and the nonlocal resistance $R_{12,34}$ are small. Denoting L_{ij} as the distances between the electrode i and j and assuming L_{12} and L_{34} are much longer than the spin relaxation length λ of the graphene in the normal state, the nonlocal resistance $R_{12,34}$ can be obtained analytically[34]: $R^{\rm normal}_{12,34} = \frac{1}{2}P^2\frac{\lambda}{\sigma_G W}e^{-L_{23}/\lambda}$, where W is the width of the graphene ribbon, P is the spin polarization of the FM electrode, and σ_G is the conductivity of normal FM graphene. On the other hand, when FM graphene is in the spin superconductor phase, the spin resistance is zero and the spin current can flow through it with no dissipation. In this case, the nonlocal resistance can be obtained as $R^{\rm SSC}_{12,34} = \frac{1}{2}P^2\frac{\lambda}{\sigma_G W}e^{-(L_{23}-L_{\rm SSC})/\lambda} = R^{\rm normal}_{12,34}e^{L_{\rm SSC}/\lambda}$, where $L_{\rm SSC}$ is the length of the spin superconductor. Notice $R^{\rm SSC}_{12,34}$ is much larger than $R^{\rm normal}_{12,34}$. Therefore, a sharp increase in the nonlocal resistance can be observed [see Fig. 4(c)] when the temperature T varies from $T > T_C$ to $T < T_C$. In addition, because the spin superconductor is an (charge) insulator, a sharp increase can also be observed in the resistance R_{23} between electrodes 2 and 3 [see Fig. 4(d)], as discussed above in point 2.

VI. CONCLUSION

In conclusion, we predict a spin superconductor state in the FM graphene at the low temperature, as the counterpart to the (charge) superconductor state. The spin superconductor can carry the dissipationless spin supercurrent at equilibrium, and its spin resistance is zero. A BCS-type theory for the spin superconductor was presented, and an electric Meissner effect and a spin-current Josephson effect in spin superconductor were demonstrated. We also suggest a feasible experiment setup to detect the spin superconductor.

Finally, we comment that the spin superconductor may also exist in other systems, for example, the bilayer FM graphene, some 3D FM materials, Bose-Einstein condensate of magnetic atoms, etc. Like superconductivity, spin superconductivity may also be a general phenomenon at low temperature.

ACKNOWLEDGMENTS

This work was financially supported by NSF-China under Grants No. 10734110, No. 10974015, No. 11074174, and No. 10874191, and China-973 program.

APPENDIX

In this Appendix we discuss the instability of the FM metal state in the presence of the attractive e-h interaction in detail.

Let us begin from the free Dirac fermion Hamiltonian in Eq. (1):

$$H_0 = \begin{pmatrix} -\sigma M & v_F(\hat{p}_x - i\hat{p}_y) \\ v_F(\hat{p}_x + i\hat{p}_y) & -\sigma M \end{pmatrix} = v_F \hat{\tau}\cdot\hat{\mathbf{p}} - \sigma M. \tag{A1}$$

Here $\hat{\mathbf{p}} = (\hat{p}_x, \hat{p}_y)$ is the momentum operator, $\mathbf{r} = (x, y)$ is the particle coordinates, and $\hat{\tau}$ is pseudospin Pauli matrices. For the spin-up subsystem, the Schrödinger equation is

$$(v_F\hat{\tau}\cdot\hat{\mathbf{p}} - M)\Psi_{e\uparrow}(\mathbf{r}) = E\Psi_{e\uparrow}(\mathbf{r}), \tag{A2}$$

with the eigenenergy $E = \pm v_F k - M$ and eigenstate $\Psi_{e\uparrow}(\mathbf{r}) = \frac{\sqrt{2}}{2}(\pm e^{-i\theta}, 1)^T e^{i\mathbf{k}\cdot\mathbf{r}}$. For the spin-down subsystem, the Schrödinger equation is

$$(v_F\hat{\tau}\cdot\hat{\mathbf{p}} + M)\Psi_{e\downarrow}(\mathbf{r}) = E\Psi_{e\downarrow}(\mathbf{r}), \tag{A3}$$

with the eigenenergy $E = \pm v_F k + M$ and eigenstate $\Psi_{e\downarrow}(\mathbf{r}) = \Psi_{e\uparrow}(\mathbf{r})$. Due to the spin-down carriers being hole-like [see Fig. 1(b)], we take the e-h transformation. After the e-h transformation, the Schrödinger equation of the spin-down subsystem is

$$(v_F\hat{\tau}^*\cdot\hat{\mathbf{p}} - M)\Psi_{h\uparrow}(\mathbf{r}) = E\Psi_{h\uparrow}(\mathbf{r}). \tag{A4}$$

Let us consider the free fermion system in the ground state [see Fig. 1(b)], in which two high-energy bands $\epsilon_{-\uparrow}$ and $\epsilon_{+\downarrow}$ are completely full and empty, respectively, and two low-energy bands $\epsilon_{+\uparrow}$ and $\epsilon_{-\downarrow}$ are partly filled up to $E_F = 0$ by electron and hole, respectively. This state is the usual FM metal state. Below we will show that, in the presence of an e-h attractive interaction, no matter how weak, this state becomes unstable. Following the process in Ref. 35, we consider an electron and a hole at the coordinates $\mathbf{r}_e$ and $\mathbf{r}_h$, the other electrons and holes still are treated as a free gas. The only effect of these free electrons and holes are to forbid the electron and hole to occupy all states $E < E_F = 0$ (or $v_F k < M$) by the exclusion principle. Let $\Psi_{eh}(\mathbf{r}_e, \mathbf{r}_h)$ be the two-particle wave function and consider only states where the center of the pair is at rest, then Ψ_{eh} is only a function of $\mathbf{r}_e - \mathbf{r}_h$ and it can be expanded as

$$\Psi_{eh}(\mathbf{r}_e, \mathbf{r}_h) = \sum_{\mathbf{k}} g_{\mathbf{k}} \Psi^0_{e\uparrow}\Psi^0_{h\uparrow} e^{i\mathbf{k}\cdot(\mathbf{r}_e - \mathbf{r}_h)}, \tag{A5}$$

where $\Psi^0_{e\uparrow} = \frac{\sqrt{2}}{2}(e^{-i\theta}, 1)^T$ and $\Psi^0_{h\uparrow} = \frac{\sqrt{2}}{2}(-e^{i\theta}, 1)^T$. Due to the exclusion principle, the probability amplitude $g_{\mathbf{k}} = 0$ for $k < M/v_F$.

Combining Eqs. (A2) and (A4), the Schrödinger equation for two particles is

$$(v_F\hat{\tau}_e\cdot\hat{\mathbf{p}}_e + v_F\hat{\tau}^*_h\cdot\hat{\mathbf{p}}_h - 2M)\Psi_{eh} + U(\mathbf{r}_e, \mathbf{r}_h)\Psi_{eh} = E\Psi_{eh}. \tag{A6}$$

Here $U(\mathbf{r}_e, \mathbf{r}_h)$ is the attractive e-h interaction and $\hat{\tau}_e$ ($\hat{\mathbf{p}}_e$) and $\hat{\tau}_h$ ($\hat{\mathbf{p}}_h$) act on the electron and hole elements, respectively. On inserting Eq. (A5) into Eq. (A6) we have

$$(2v_F k - 2M)g_{\mathbf{k}} - \sum_{\mathbf{k}'(k'>M/v_F)} U_{\mathbf{k}\mathbf{k}'} g_{\mathbf{k}'} = E g_{\mathbf{k}}, \tag{A7}$$

where $U_{\mathbf{k}\mathbf{k}'} \equiv -\iint U(\mathbf{r}_e, \mathbf{r}_h) e^{i(\mathbf{k}-\mathbf{k}')\cdot(\mathbf{r}_e - \mathbf{r}_h)} d\mathbf{r}_e d\mathbf{r}_h$. We then obtain

$$g_{\mathbf{k}} = -\sum_{\mathbf{k}'(k'>M/v_F)} g_{\mathbf{k}'} U_{\mathbf{k}\mathbf{k}'}/(E - 2v_F k + 2M). \tag{A8}$$

Let us assume that $U_{\mathbf{k}\mathbf{k}'}$ is independent $\mathbf{k}$ and $\mathbf{k}'$, we have

$$\begin{aligned} 1 &= -U \sum_{\mathbf{k}(k_D>k>M/v_F)} \frac{1}{E - 2v_F k + 2M} \\ &= -U \int_M^{v_F k_D} d\epsilon \frac{\rho_\epsilon}{E - 2\epsilon + 2M}, \end{aligned} \tag{A9}$$

with the density of state ρ_ϵ. It is very easy to prove that Eq. (A9) has the negative E solution, as soon as U is positive and $M \neq 0$. Therefore, no matter how weak attractive e-h interaction U and the value of k_D, there always exists an e-h bound state with the energy $E < 0$. The usual FM metal state is thus unstable.

Finally, we also emphasize that there only exists two bands, spin-up electron band and spin-up hole band, on the Fermi surface in the FM graphene. So the two particle bound state is only between the electron and hole, and it cannot be between two electrons (or two holes). So the spin superconducting instability is the sole instability.

*sunqf@aphy.iphy.ac.cn

[1] H. K. Onnes, Leiden Comm. **122**b, **122**c (1911); for a text book see D. Shoenberg, *Superconducting* (Cambridge University Press, Cambridge, 1952).

[2] W. Meissner and R. Ochsenfeld, Naturwiss **21**, 787 (1933).

[3] B. D. Josephson, Phys. Lett. **1**, 251 (1962).

[4] S. A. Wolf, D. D. Awschalom, R. A. Buhrman, J. M. Daughton, S. V. Molnar, M. L. Roukes, A. Y. Chtchelkanova, and D. M. Treger, Science **294**, 1488 (2001); G. A. Prinz, *ibid.* **282**, 1660 (1998).

[5] J. Bardeen, L. N. Cooper, and J. R. Schrieffer, Phys. Rev. **108**, 1175 (1957).

[6] E. Hanamura and H. Haug, Phys. Rep. **33**, 209 (1977).

[7] A review on the exciton can be found in S. A. Moskalenko and D. W. Snoke, *Bose-Einstein Condensation of Excitons and Biexcitons: and Coherent Nonlinear Optics With Excitons* (Cambridge University Press, Cambridge, 2000).

[8] B. Deveaud, F. Clerot, N. Roy, K. Satzke, B. Sermage, and D. S. Katzer, Phys. Rev. Lett. **67**, 2355 (1991).

[9] J. Feldmann, G. Peter, E. O. Göbel, P. Dawson, K. Moore, C. Foxon, and R. J. Elliott, Phys. Rev. Lett. **59**, 2337 (1987).

[10] R. Rapaport and G. Chen, J. Phys. Condens. Matter **19**, 295207 (2007).

[11] S. I. Shevchenko, Fiz. Nizk. Temp. **2**, 505 (1976) [Sov. J. Low Temp. Phys. **2**, 251 (1976)].

[12]Yu. E. Lozovik and V. I. Yudson, JETP Lett. **22**, 274 (1975); Solid State Commun. **19**, 391 (1976).
[13]U. Sivan, P. M. Solomon, and H. Shtrikman, Phys. Rev. Lett. **68**, 1196 (1992).
[14]L. V. Butov, A. Zrenner, G. Abstreiter, G. Böhm, and G. Weimann, Phys. Rev. Lett. **73**, 304 (1994); M. Bayer, V. B. Timofeev, F. Faller, T. Gutbrod, and A. Forchel, Phys. Rev. B **54**, 8799 (1996).
[15]K. S. Novoselov, A. K. Geim, S. V. Morozov, D. Jiang, Y. Zhang, S. V. Dubonos, I. V. Grigorieva, and A. A. Firsov, Science **306**, 666 (2004); K. S. Novoselov, A. K. Geim, S. V. Morozov, D. Jiang, M. I. Katsnelson, I. V. Grigorieva, S. V. Dubonos, and A. A. Firsov, Nature (London) **438**, 197 (2005); Y. Zhang, Y.-W. Tan, H. L. Stormer, and P. Kim, *ibid.* **438**, 201 (2005).
[16]N. Tombros, C. Jozsa, M. Popinciuc, H. T. Jonkman, and B. J. van Wees, Nature (London) **448**, 571 (2007).
[17]C. W. J. Beenakker, Rev. Mod. Phys. **80**, 1337 (2008); A. H. Castro Neto, F. Guinea, N. M. R. Peres, K. S. Novoselov, and A. K. Geim, *ibid.* **81**, 109 (2009).
[18]N. M. R. Peres, Rev. Mod. Phys. **82**, 2673 (2010).
[19]C.-H. Zhang and Y. N. Joglekar, Phys. Rev. B **77**, 233405 (2008); H. Min, R. Bistritzer, J.-J. Su, and A. H. MacDonald, *ibid.* **78**, 121401 (2008); B. Seradjeh, H. Weber, and M. Franz, Phys. Rev. Lett. **101**, 246404 (2008).
[20]M. Yu. Kharitonov and K. B. Efetov, Phys. Rev. B **78**, 241401(R) (2008).
[21]M. P. Mink, H. T. C. Stoof, R. A. Duine, and A. H. MacDonald, Phys. Rev. B **84**, 155409 (2011).
[22]D. V. Khveshchenko, Phys. Rev. Lett. **87**, 206401 (2001); **87**, 246802 (2001).
[23]I. L. Aleiner, D. E. Kharzeev, and A. M. Tsvelik, Phys. Rev. B **76**, 195415 (2007).
[24]H. Haugen, D. Huertas-Hernando, and A. Brataas, Phys. Rev. B **77**, 115406 (2008); J. Linder, T. Yokoyama, D. Huertas-Hernando, and A. Sudbo, Phys. Rev. Lett. **100**, 187004 (2008).
[25]Q. Zhang, D. Fu, B. Wang, R. Zhang, and D. Y. Xing, Phys. Rev. Lett. **101**, 047005 (2008).
[26]Y.-W. Son, M. L. Cohen, and S. G. Louie, Nature (London) **444**, 347 (2006); E.-J. Kan, Z. Li, J. Yang, and J. G. Hou, Appl. Phys. Lett. **91**, 243116 (2007).
[27]D. A. Abanin, S. V. Morozov, L. A. Ponomarenko, R. V. Gorbachev, A. S. Mayorov, M. I. Katsnelson, K. Watanabe, T. Taniguchi, K. S. Novoselov, L. S. Levitov, and A. K. Geim, Science **332**, 328 (2011).
[28]F. London and H. London, Proc. R. Soc. London Ser. A**155**, 71 (1935).
[29]Q.-F. Sun, H. Guo, and J. Wang, Phys. Rev. B **69**, 054409 (2004); Q.-F. Sun and X. C. Xie, *ibid.* **72**, 245305 (2005).
[30]Q.-F. Sun, B.-G. Wang, J. Wang, and T.-H. Lin, Phys. Rev. B **61**, 4754 (2000).
[31]Q.-F. Sun, J. Wang, and T.-H. Lin, Phys. Rev. B **59**, 3831 (1999); **59**, 13126 (1999).
[32]J. Wang, B. F. Zhu, and R. B. Liu, Phys. Rev. Lett. **104**, 256601 (2010); L. K. Werake and H. Zhao, Nat. Phys. **6**, 875 (2010).
[33]Y. K. Kato, R. C. Myers, A. C. Gossard, and D. D. Awschalom, Science **306**, 1910 (2004); S. M. Frolov, S. Lüscher, W. Yu, Y. Ren, J. A. Folk, and W. Wegscheider, Nature (London) **458**, 868 (2009).
[34]F. J. Jedema, H. B. Heersche, A. T. Filip, J. J. A. Baselmans, and B. J. van Wees, Nature (London) **416**, 713 (2002); S. O. Valenzuela and M. Tinkham, *ibid.* **442**, 176 (2006).
[35]L. N. Cooper, Phys. Rev. **104**, 1189 (1956); P. G. de Gennes and P. A. Pincus, *Superconductivity of Metals and Alloys* (Addison-Wesley, Reading, PA, 1989), pp. P93–P95.